THE JOURNAL OF BIOLOGICAL CHEMISTRY
Vol. 278, No. 5, Issue of January 31, pp. 2792–2798, 2003
Printed in U.S.A.

Structure-Function Analysis of Invasion Plasmid Antigen C (IpaC) from *Shigella flexneri**

Received for publication, August 16, 2002, and in revised form, November 7, 2002
Published, JBC Papers in Press, November 8, 2002, DOI 10.1074/jbc.M208383200

Lisa A. Kueltzo‡§¶, John Osiecki§‖, Jeff Barker‖, Wendy L. Picking‖, Baran Ersoy‡, William D. Picking‖‡‡, and C. Russell Middaugh‡**

From the Departments of ‡Pharmaceutical Chemistry and ‖Molecular Biosciences, University of Kansas, Lawrence, Kansas 66045

***Shigella flexneri* causes a self-limiting gastroenteritis in humans, characterized by severe localized inflammation and ulceration of the colonic mucosa. Shigellosis most often targets young children in underdeveloped countries. Invasion plasmid antigen C (IpaC) has been identified as the primary effector protein for *Shigella* invasion of epithelial cells. Although an initial model of IpaC function has been developed, no detailed structural information is available that could assist in a better understanding of the molecular basis for its interactions with the host cytoskeleton and phospholipid membrane. We have therefore initiated structural studies of IpaC, IpaC I′, (residues 101–363 deleted), and IpaC ΔH (residues 63–170 deleted). The secondary and tertiary structure of the protein was examined as a function of temperature, employing circular dichroism and high resolution derivative absorbance techniques. ANS (8-anilino-1-napthalene sulfonic acid) was used to probe the exposure of the hydrophobic surfaces under different conditions. The interaction of IpaC and these mutants with a liposome model (liposomes with entrapped fluorescein) was also examined. Domain III (residues 261–363) was studied using linker-scanning mutagenesis. It was shown that domain III contains periodic, sequence-dependent activity, suggesting helical structure in this section of the protein. In addition to these structural studies, investigation into the actin nucleation properties of IpaC was conducted, and actin nucleation by IpaC and some of the mutants was exhibited. Structure-function relationships of IpaC are discussed.**

Shigella flexneri causes a self-limiting gastroenteritis called shigellosis, which is characterized by severe localized inflammation and ulceration of the colonic mucosa (1). An estimated 360,000 *Shigella* cases occur in the United States each year, although only 18,000 are reported (2). In developing countries, the disease is present in most villages. It most commonly strikes young children and is responsible for an estimated 600,000 deaths/year worldwide (all *Shigella spp.* combined) (1). Shigellosis onset involves bacterial invasion of intestinal epithelial cells by a process called "pathogen-induced phagocytosis" (2, 3) and requires the expression of the *ipa* operon. The invasion plasmid antigens (or Ipa[1] proteins) are effector proteins that are exported by a dedicated type III secretion system (TTSS) at the host-pathogen interface. There they directly interact with the host cell to promote actin cytoskeleton rearrangements at the site of bacterial contact (2). These cytoskeletal changes give rise to filopodia, which mature into membrane ruffles that coalesce to trap the pathogen within a membrane-bound vacuole (2). The vacuole is then quickly lysed to provide the bacterium with access to the host cytoplasm, where it proliferates and is able to directly invade neighboring cells (4).

IpaC has been identified as the primary effector protein for *Shigella* invasion of epithelial cells (5–8). Effector-related functions described for purified IpaC include: (*a*) enhanced invasion of cultured cells by *S. flexneri* (5, 8, 9); (*b*) induced uptake of virulence plasmid-cured *S. flexneri* (5); (*c*) interaction with phospholipid membranes (9–11); and (*d*) triggering of cytoskeletal changes in cultured cells (7, 9, 12). Additional activities associated with IpaC include oligomerization in solution (8), reconstitution into complexes with IpaB *in vitro* (8), *in vivo* formation of complexes containing IpaB that promote the uptake of latex beads by cultured cells (6), and reconstitution with IpaB and IpaD to form a complex that may allow entry of noninvasive *Escherichia coli* into cultured cells (13).

It has been demonstrated that IpaC possesses a distinct functional organization (Scheme I). The immediate N terminus of IpaC is required for secretion, whereas a region near the N terminus is responsible for association with IpaB, which is probably needed for proper presentation of IpaC to the target cell membrane. The central hydrophobic region of IpaC directs IpaC penetration of phospholipid membranes and contributes to interactions with IpaB (14).[2] The ability of IpaC to interact with phospholipid membranes does not require secretion by the TTSS of *S. flexneri* (Ref. 9 and this work); however, active insertion of IpaC into target cell membranes by the TTSS greatly increases the efficiency of this process (15). The C terminus of IpaC mediates IpaC-IpaC interactions and probably possesses IpaC effector function (7, 14). This information, however, only provides a very general picture of IpaC structure and function and its role in the *S. flexneri* infection process.

* This work was supported by an NIGMS, National Institutes of Health Biotechnology Training Grant to the University of Kansas, a Bristol Myers Squibb tuition fellowship (to L. A. K.), and NIAID, National Institutes of Health funding (Grant AI34428) to (W. D. P.). The costs of publication of this article were defrayed in part by the payment of page charges. This article must therefore be hereby marked "*advertisement*" in accordance with 18 U.S.C. Section 1734 solely to indicate this fact.

§ These authors contributed equally to this work.
¶ Present address: University of Colorado Health Sciences Center, School of Pharmacy, 4200 E. 9th Ave., Denver, CO, 80262.
** Present address: Dept. of Molecular Microbiology, University of Texas at San Antonio, Health Science Center, San Antonio, TX 78229.
‡‡ To whom correspondence should be addressed. Tel.: 785-864-3299; Fax: 785-864-5294; E-mail picking@ku.edu.

[1] The abbreviations used are: Ipa, invasion plasmid antigens; IpaC, invasion plasmid antigen C; IpaD, invasion plasmid antigen D; ANS, 8-anilino-1-napthalene sulfonic acid; TTSS, type III secretion system; MEM, minimum Eagle's medium; SipC, *Salmonella* invasion protein C.
[2] A. Harrington and W. Picking, manuscript in preparation.

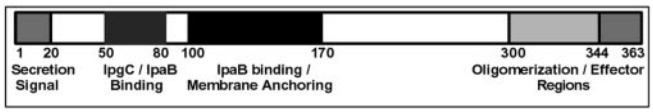

SCHEME 1. **Functional organization of IpaC.** The N terminus of IpaC harbors sequences for TTSS export and interaction with IpgC and IpaB. The central hydrophobic region is involved in IpaB binding, IpaC penetration of phospholipid membranes, and possibly protein stabilization. The C terminus possesses essential oligomerization and effector functions. Residues 101–363 are deleted in IpaC I′ ,and residues 63–170 are deleted in IpaC ΔH.

Unfortunately, there exists no detailed structural information concerning IpaC that could provide a molecular basis for its interactions with the host cytoskeleton and phospholipid membranes.

In this work, we have initiated studies into the structure of IpaC by employing a number of biophysical approaches. Truncated versions of IpaC, specifically IpaC I′ (residues 101–363 deleted) and IpaC ΔH (residues 63–170 deleted), were overexpressed in *E. coli* and purified, permitting structural analysis and a more comprehensive investigation into the role of the individual domains described above. The interaction of these mutants and full-length IpaC with a liposome model was also examined. In addition to these structural studies, an investigation into the actin nucleation properties of IpaC and these deletion constructs was conducted. Finally, domain III (residues 261–363), which has previously resisted attempts at purification after recombinant expression, was studied using an alternate technique, linker-scanning mutagenesis. From this, it is shown that domain III contains a sequence periodic structure-activity relationship, which suggests that the activity may be dependent on helical structure in this region. Interpretation of IpaC structure with regard to the functional properties of the wild-type protein is then discussed.

EXPERIMENTAL PROCEDURES

Materials—DOPC (dioleoylphosphatidylcholine) and DOPG (dioleoylphosphatidylglycerol) were purchased from Avanti. ANS (8-anilino-1-naphthalene sulfonic acid) was obtained from Across Organics, and fluorescein (5,6-carboxyfluorescein, high purity) was obtained from Molecular Probes. Dialysis materials were provided by Spectra. All other chemicals were of reagent grade and obtained from Sigma and Fisher.

Preparation of Affinity-purified Recombinant Proteins—Plasmids used to prepare recombinant IpaC and IpaC ΔH and sipC have been described previously (5, 16, 17). pWPI′ was designed to encode an IpaC peptide called region I′, in which residues 101–363 are deleted. This plasmid was generated as pWPC15 except that the 3′ primer was designed to place a stop codon at amino acid 101. All new plasmids were transformed into *E. coli* BL21(DE3) for high level protein expression. Recombinant proteins were purified via the N-terminal His_6 tag by nickel chelation chromatography under denaturing conditions as described in detail previously (5, 14, 17). Purified proteins were step-dialyzed against 10 mM $NaPO_4$, pH 7.2, 150 mM NaCl containing 0.5 mM dithiothreitol to remove the urea.

Sample Preparation—Purified proteins in buffer were stored at −70 °C for long term storage (IpaC only) or 4 °C for short term use (<2 weeks). All protein samples were centrifuged at 13,400 × *g* for 5 min at 4 °C on the day of use to remove aggregates formed during storage. Tween 20 (0.1%) was added to the IpaC solutions to further stabilize them during freezing. Unfortunately, neither centrifugation nor filtration was effective at completely removing all aggregated material (observed as a small amount of optical density above 300 nm in absorbance spectra). Concentrations were therefore obtained employing derivative absorbance spectroscopy, using *N*-acetyl-L-tyrosine-ethyl ester derivative minima at 275 and 283 nm to establish a standard curve since IpaC possesses no tryptophan residues. Biophysical studies were conducted in 10 mM $NaPO_4$, 150 mM NaCl, pH 7.2, containing 1 mM dithiothreitol.

Circular Dichroism—CD spectra were recorded with a Jasco J-720 spectrophotometer (Tokyo, Japan) equipped with a Peltier temperature controller. Far UV spectra (between 195 and 260 nm) were collected using a 1-mm path length cuvette sealed with a Teflon stopper. A resolution of 0.1 nm and a scanning speed of 20 nm/min with a 2-s response time were employed. Spectra presented are an average of six consecutive spectra. Spectra were recorded at 5 °C intervals employing a thermostated cuvette holder. An incubation time of 3 min at each temperature interval (sufficient for equilibrium to be obtained) and a temperature ramp rate of 20 °C/h were employed. Protein concentrations of 8.3, 26.3, and 11.2 μM were employed for IpaC, IpaC I′, and IpaC ΔH, respectively. Noise reduction and data analysis were performed using Standard Analysis and Temperature/Wavelength Analysis programs (Jasco) and MicroCal Origin™ 6.0 software. Secondary structure content was estimated using the CONTIN (18), SELCON (19), and CDSSTR (20) analysis programs provided with the CDPro software suite (21).

Derivative Absorbance Spectroscopy—High-resolution absorbance spectra were collected on a Hewlett-Packard 8453 UV-Visible spectrophotometer (Agilent, Palo Alto, CA) fitted with a Peltier temperature controller. Temperature perturbation studies were conducted at protein concentrations of 12.7, 25.3, and 16.9 μM for IpaC, IpaC I′, and IpaC ΔH, respectively. Spectra were collected for 25 s at 2.5 °C intervals with a 3-min equilibration time before collection of each spectrum. Spectral analysis was conducted using UV-Visible Chemstation software (Agilent) and Microcal Origin™ 6.0. Second derivative spectra were calculated employing a nine-point data filter and fifth degree Savitzky-Golay polynomial and subsequently fitted to a cubic function with 99 interpolated points/raw data point, permitting 0.01-nm resolution (22). Peak positions were then determined from the interpolated curves. Optical density data were simultaneously monitored at 350 nm.

Lipid Interaction Studies—Aliquots of DOPC and DOPG in chloroform were dried under nitrogen and vacuum to create thin films of either 100% DOPC or 50:50 [DOPC]:[DOPG]. Films were hydrated in a solution containing 100 mM 5,6-carboxyfluorescein at pH 7.0 in water for 10 min and then sonicated in a bath sonicator for 30 min prior to extrusion through a 100-nm pore size membrane 10 times at 45 °C. A final size of ~150 nm was determined with a Brookhaven ZetaPALS dynamic light scattering instrument (Holtsville, NY) equipped with a 25 mW 626-nm laser. Excess dye was separated from the bulk liposomes by size exclusion chromatography, employing a Sephadex G-25 column coupled to an AKTA FLPC (Amersham Biosciences). The run buffer was 10 mM $NaPO_4$, 150 mM NaCl, pH 7.4. Peak fractions were collected and pooled, and lipid content was determined by a total phosphorous assay, as described (23). Solutions were stored at 4 °C and protected from light.

Time-based release studies were conducted with a PTI QuantaMaster spectrophotometer with a thermostated cuvette holder. Samples were excited at 492 nm, and the emission signal was monitored at 517 nm for 10 min. Excitation slits were set at 1 nm, and emission was set at 2 nm. Data points were collected at 0.2-s intervals. Data were collected as follows: buffer was incubated for 3 min at the desired temperature prior to adding liposome solutions. Baseline fluorescence was monitored with liposomes alone for 10 min to determine residual release of fluorescein from the liposomes. Maximum fluorescein release, as defined by release in the presence of 0.1% Triton, was determined by adding Triton to the liposome solution 3 min after the start of signal collection. Protein-induced fluorescein release was examined by monitoring the fluorescein signal at 512 nm after addition of protein to the liposome solution after 3 min of incubation. Both protein and Triton solutions were added during continuous signal collection through a syringe port in the sample compartment. The protein concentration employed was 1 μM, and the total lipid concentration was 100 μM. Release was monitored at 10, 20, 30, 35, 40, 45, 50, and 60 °C. Samples were measured in triplicate. The extent of release was calculated as a percentage of Triton-induced release at 600 s after background correction. Analysis was conducted using Felix (PTI) and MicroCal Origin™ software.

Assay for Actin Nucleation—The fluorescence of pyrene-labeled G-actin monomers increases following assembly into pyrene F-actin (24). For monitoring IpaC-mediated actin nucleation *in vitro*, pyrene G-actin was incubated at 4 °C in G-actin buffer (5 mM Tris-HCl, pH 8.0, 0.1 mM ATP, 0.2 mM $CaCl_2$). Test protein (IpaC or an IpaC mutant) was then added to the sample, and pyrene fluorescence was monitored at 23 °C. A Spex FluoroMax instrument (Jobin Yvon Horiba, Edison, NJ) was used to measure pyrene fluorescence using a time-based acquisition mode with an excitation wavelength of 330 and an emission wavelength of 385 nm. After 15 min, 50× actin polymerization buffer (100 mM $MgCl_2$, 50 mM ATP, 2.5 M KCl) was added, and the change in pyrene fluorescence was monitored as a function of time. Negative controls either contained no added protein or contained IpaD, which has no actin-nucleating activity. SipC from *Salmonella typhimurium*, which

has been shown to nucleate actin *in vitro*, was used as a positive control (24).

Linker-scanning Mutagenesis—Linker-scanning mutagenesis was used to introduce consecutive site-specific mutations into a predicted coiled-coil segment near the C terminus of IpaC. Either *Nhe*I cleavage sites encoding Ala-Ser pairs or *Xho*I sites encoding Leu-Glu pairs were generated throughout the length of the putative coiled-coil region (amino acids 309–344). Primers with a 5′ *Nhe*I or *Xho*I site and the appropriate neighboring *ipaC* sequences running in either direction were used for inverse PCR. The product was digested with *Nhe*I or *Xho*I, respectively, and then ligated. The resulting plasmids were electroporated into the *S. flexneri* IpaC mutant strain SF621, and the ability to restore invasion and contact hemolysis functions was determined as described below.

S. flexneri Invasion of Cultured Cells and Contact-mediated Hemolysis—*S. flexneri* invasion of Henle 407 cells was monitored using a standard gentamycin protection assay as described (16). Semiconfluent monolayers of Henle 407 cells were seeded into 24-well plates and grown overnight. SF621 harboring the desired plasmid was grown in trypticase soy broth containing 100 μg/ml ampicillin and 50 μg/ml kanamycin to an A_{600} of 0.4–0.6. The bacteria were diluted with serum-free MEM containing 0.45% glucose (MEM-glc), centrifuged onto the surface of semiconfluent Henle 407 monolayers, and incubated with the cells for 30 min at 37 °C. Free bacteria were removed by aspiration, and the cells were washed with MEM containing 5% calf serum and 50 μg/ml gentamycin. The cells were incubated in the final gentamycin wash for 2 h (to kill adherent, noninternalized bacteria) and rinsed with MEM-glc. The cells were lysed by overlaying them with 250 μl of 0.5% agarose in water. The agarose was then overlaid with 0.5% agar containing 2× LB medium. After overnight incubation at 37 °C, internalized bacteria formed subsurface colonies that were quantified using a ChemiImager 4400 system (Alpha Innotech Corp., San Leandro, CA).

RESULTS

Statistics—All errors are reported as standard error (S.E., $n = 3$) unless otherwise indicated.

Spectroscopic Analysis of Full-length IpaC, IpaC I′, and IpaC ΔH—To better understand the function of IpaC in the *S. flexneri* invasion process, a series of structural studies were conducted to characterize the secondary and tertiary structure of full-length IpaC, IpaC I′, and ΔH mutants and their response to temperature. All three proteins are efficiently secreted by the *S. flexneri* SF621 TTSS and are able to interact with IpaB, indicating that biological functions associated with the N terminus remain intact (14).

The CD spectrum of IpaC at 20 °C exhibits minima at 222 and 204 nm, suggesting the presence of some helical structure (Fig. 1*A*). Secondary structure estimates indicate that IpaC contains a mixture of α-helical and β-sheet structure with significant turn and random structure also present (Table I). In contrast, IpaC I′ and IpaC ΔH appear to be less structured, as indicated by a decrease in CD intensity above 210 nm. The spectrum of IpaC I′ exhibits an increase in negative intensity near 200 nm, suggesting increased random structure. Solution conditions prevented collection of data below 200 nm, preventing secondary structure estimation for both mutants. IpaC undergoes a significant change in secondary structure at fairly moderate temperatures (Table I and Fig. 1). This transition suggests a loss of helix content (Table I) and has a midpoint of 43.3 ± 0.3 °C ($n = 3$). In contrast, IpaC I′ and IpaC ΔH display evidence of only weak transitions between 10 and 40 °C. Although limited aggregation of some samples was observed above 30 °C, no red shifts or strong decreases in intensity indicative of absorption flattening were observed, indicating that the spectral changes are not an artifact of aggregation-dependent phenomena.

Because IpaC lacks tryptophan residues, derivative absorbance spectroscopy was employed to monitor tertiary structure changes. This method is especially useful in aggregating systems since it is not sensitive to broad spectral components such as light scattering (25). The spectra display two phenylalanine

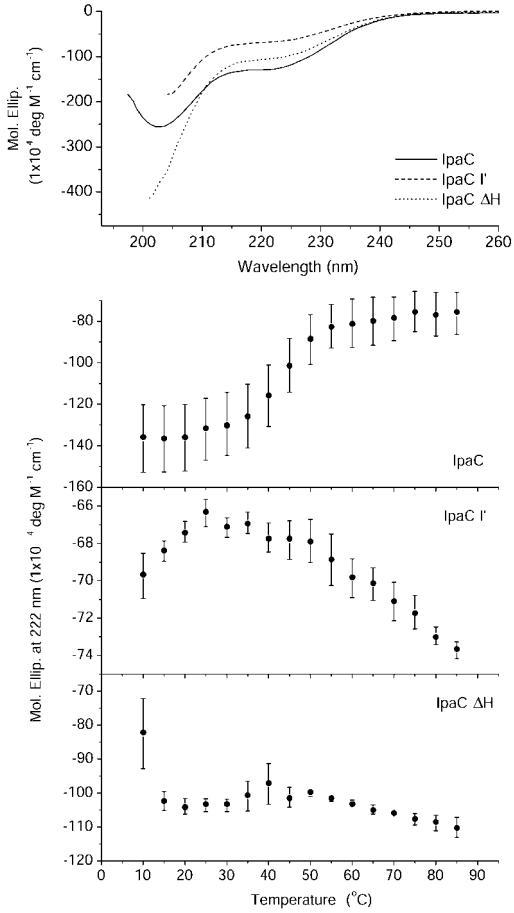

FIG. 1. **Circular dichroism analysis of IpaC and its mutants.** *A*, CD spectrum of IpaC and mutants at 20 °C. Protein concentrations were 8.3, 26.3, and 11.2 μM for IpaC, IpaC I′, and IpaC ΔH, respectively. Spectra were collected at a rate of 20 nm/min employing a resolution of 2 nm. Spectra presented are an average of three consecutive spectra. The buffer used was 10 mM phosphate, 150 mM NaCl, and 1 mM dithiothreitol, pH 7.2. *B–D*, temperature dependence of the molar ellipticity at 222 nm of IpaC, IpaC I′, and IpaC ΔH. A major loss in ellipticity is observed for the full-length IpaC with a T_m of 43.3 ± 0.3 ($n = 3$). Spectra were recorded at 5 °C intervals employing an incubation time of 3 min at each temperature interval and a temperature ramp rate of 20 °C/h. All other experimental conditions are as in *panel A*.

TABLE I
Secondary structure estimates for IpaC

Temperature	α-Helix	β-Sheet	Turn	Random
	%	%	%	%
20 °C	10 (2)[a]	34 (1)	22 (2)	32 (2)
40 °C	7 (1)	35 (2)	23 (2)	35 (1)
60 °C	4 (0)	38 (2)	23 (2)	33 (0)

[a] Errors are reported as S.E., $n = 3$.

(Fig. 2, *A* and *B*, 253 and 260 nm) and three tyrosine (Fig. 2, *C–E*, 268, 276, and 285 nm) minima (22). Most plots of peak position *versus* temperature show similar linear increases with temperature, which is an intrinsic property of the aromatic amino acids.[3]

However, deviations from these linear plots consistent with structural alterations are observed in many cases. The IpaC Phe minimum at 253 nm is shifted to longer wavelengths relative to the two mutants and shows no temperature dependence at lower temperatures. Upon reaching the temperature at which the protein begins aggregating, the noise in the data

[3] L. A. Kueltzo and C. R. Middaugh, manuscript in preparation.

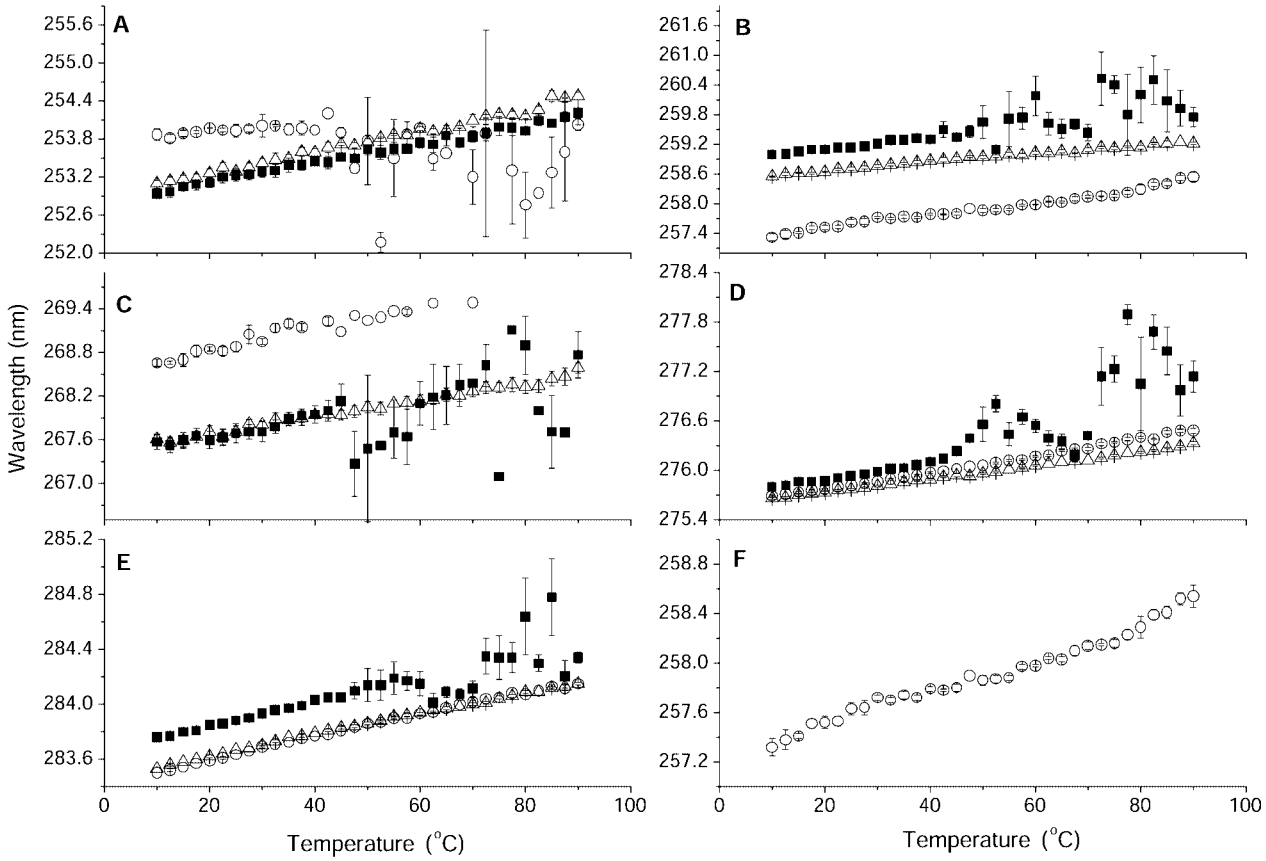

FIG. 2. **Wavelength of the derivative absorbance peaks of IpaC and mutants as a function of temperature.** Second derivative absorbance minima arising from phenylalanine (*A* and *B*) and tyrosine (*C–E*) residues. IpaC (*closed squares*), IpaC I′ (*open circles*), and IpaC ΔH (*open triangles*) are shown. *F*, expanded view of phenylalanine peak 2 position for IpaC I′ showing a subtle deviation from linearity between ~30 and 60 °C. Protein concentrations were 12.7, 25.3, and 16.9 μM for IpaC, IpaC I′, and IpaC ΔH, respectively. Spectra were collected for 25 s at 2.5 °C intervals with a 3-min equilibration time before collection of each spectrum. *Error bars* that are not visible are buried within the *symbol*.

begins to increase. The second Phe minimum shows a difference in minimum position for each of the proteins with the IpaC peak once again at the longest wavelength. An expanded version of the IpaC I′ data (Fig. 2*F*) shows that IpaC I′ actually undergoes a small but very reproducible transition between 30 and 55 °C. The 267 nm IpaC I′ tyrosine minimum is observed at longer wavelengths, disappearing from the derivative spectrum at temperatures above 62 °C. Two strong transitions are observed in the plot of the 276-nm tyrosine minimum of IpaC with no similar transitions seen for either mutant. The 284-nm IpaC I′ and IpaC ΔH tyrosine minima again manifest no evidence of conformational change, whereas the IpaC absorption band shows evidence of the two transitions and is again present at a longer wavelength (Fig. 2*E*).

Trends in protein-associative behavior can be seen by monitoring the turbidity (OD) at 350 nm as the temperature is increased (Fig. 3). Full-length IpaC shows a large change in turbidity starting near 30 °C. Transitions are observed between 30 and 70 °C and above 70 °C. Although the changes are small, a distinct transition is observed starting at 55 °C for IpaC I′, whereas IpaC ΔH shows a small but steady increase in OD starting at 20 °C (Fig. 3, *bottom panels*). Both results are consistent with the formation of soluble aggregates.

Full-length IpaC but Not the IpaC Mutants Interacts with Liposomes—The effect of IpaC, IpaC I′, and IpaC ΔH upon fluorescein-containing liposomes was examined as a function of the temperature and lipid composition. Fluorescein can be sequestered in liposomes at concentrations that produce self-

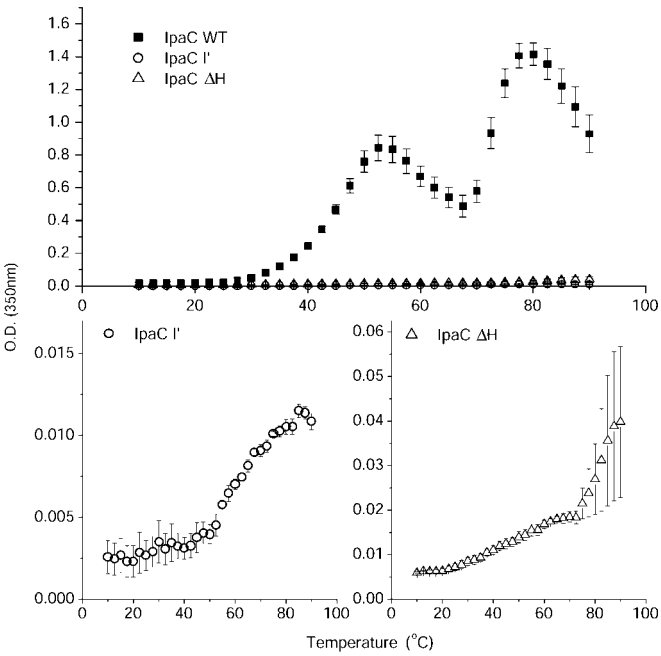

FIG. 3. **Turbidity of ipaC and mutants as a function of temperature.** *Top*, IpaC, IpaC I′, and IpaC ΔH. *WT*, wild type. *Bottom*, expanded view of IpaC I′ and IpaC ΔH. Experimental conditions are described in the legend for Fig. 2.

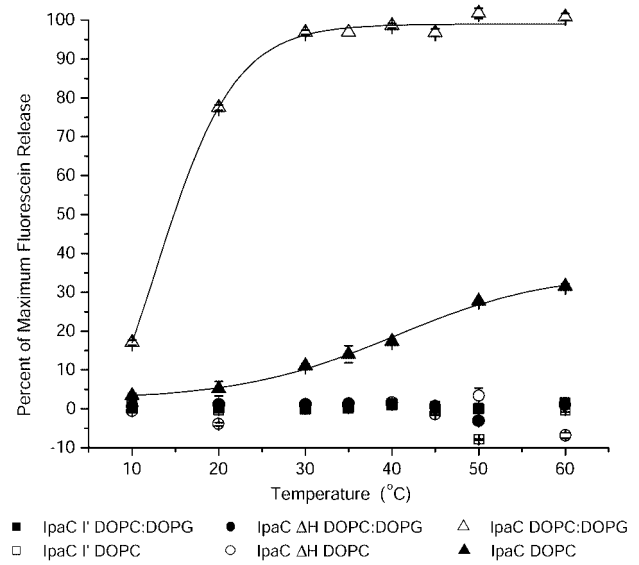

FIG. 4. **Release of fluorescein from liposomes after interaction with IpaC and mutants at various temperatures.** Release is measured as percentage of maximum release in the presence of 0.1% Triton. Protein concentration was 1 μM for all cases, and total lipid concentration is 100 μM. Liposomes were comprised of 100% DOPC or a 50:50 molar mix of DOPC and DOPG.

quenching (26). Any interaction of a protein with such loaded liposomes that is sufficient to significantly perturb the bilayer should cause a leakage of the fluorescein, leading to its dilution and an increase in the fluorescence intensity of the fluorescein dye. Using this approach, two types of vesicles were employed: 100% DOPC, producing a neutral surface charge, and 50:50 [DOPC]:[DOPG] to produce an overall negatively charged surface.

The extent of dye release at 600 s at different temperatures is shown in Fig. 4. No release is observed for IpaC I′ and IpaC ΔH. IpaC shows little release at low temperatures with DOPC liposomes, but a dramatic increase is observed at 30 °C and higher. Release at lower temperatures is greater with DOPC:DOPG liposomes. The rate of release is similar to that of the Triton control (results not illustrated). The liposomes remained above the phase transitions of the component lipids (−20 and −18 °C for DOPC and DOPG, respectively (27)) under all conditions examined.

Linker-scanning Mutagenesis Indicates That the IpaC C Terminus Is Important for Directing Uptake by Cultured Cells—The region between amino acids 309 and 344 of IpaC is predicted to possess a coiled-coil trimerization domain based on primary structure analysis (28). Attempts to purify a recombinant form of this region have been unsuccessful, so a structural analysis of this region was conducted using linker-scanning mutagenesis. Initially, *Xho*I linkers were used to substitute Leu-Glu amino acid pairs for existing amino acids in this region of IpaC. Sequence periodicity in the generation of inactivating mutations with respect to restoring invasiveness to *S. flexneri* SF621 was consistent with the presence of a coiled α-helix in this region (Fig. 5*A*). Although linker-scanning mutations near the C-terminal end of the putative coiled-coil show periodicity in reducing invasiveness, they do not eliminate IpaC activity completely. In contrast, when *Nhe*I linkers (encoding Ala-Ser) were introduced into the same region, substitution for the Leu^{335}-Ile^{336} pair did completely eliminate IpaC invasion function, as did substitution for Leu^{339}-Leu^{340} (Fig. 5*B*). This difference in the effect of amino acid substitutions at this location could be explained by the fact that the Leu-Glu led to the replacement of a nonpolar pair of amino acids by a nonpolar/

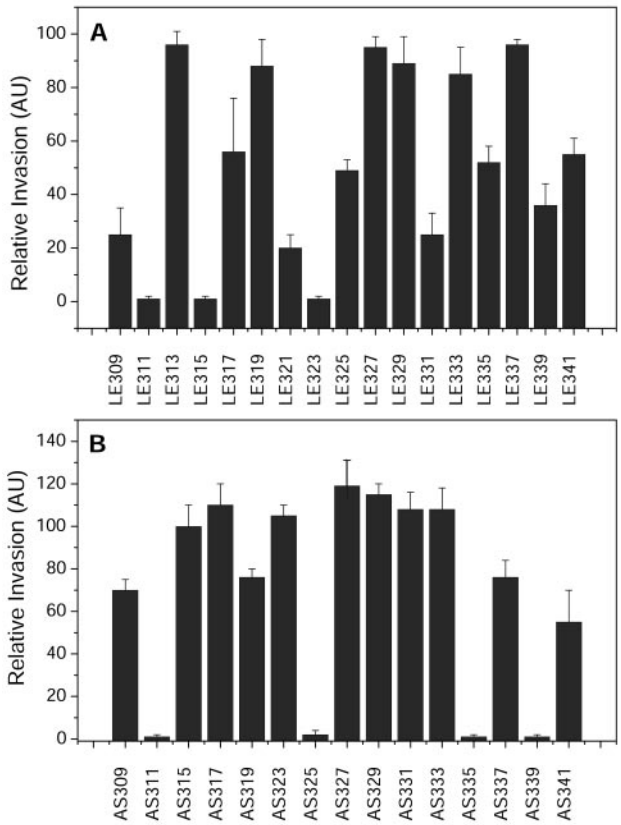

FIG. 5. **Linker-scanning mutagenesis of the putative coiled-coil region of IpaC.** In *A*, Leu-Glu amino acid pairs, encoded by *xhoI* restriction sites, were used to replace existing amino acids. In each case, the *number* given is that of the first amino acid being replaced. In *B*, the same experiment was carried out using *nheI* restriction sites, which encode Ala-Ser pairs. AS313 and AS321 were not generated because the *nheI* site would have replaced codons already specific for Ala-Ser pairs. Invasion is shown relative to that directed by native IpaC using a standard gentamycin protection assay. The data shown are the average of triplicates ± S.E.

polar pair. On the other hand, *Nhe*I scanning results in the replacement of nonpolar residues by a polar pair. In total, these data are consistent with the presence of an α-helix within this portion of IpaC.

Because a single amino acid change at Ile^{336} and Leu^{340} in the putative IpaC coiled region only partially reduced the ability of IpaC to restore invasiveness, other single amino acid changes were introduced, using Pro as the substituted amino acid because of its incompatibility with α-helix formation. When Pro was used to replace Ser^{314} at the N terminus of the putative IpaC coil, invasion function was not affected. Replacement of Lys^{326} reduced IpaC invasion function to less than half that of native IpaC (Table II). When Ile^{336} was replaced with Pro, however, IpaC invasion function was reduced more than 80% (Table II). During linker-scanning analysis, the equivalent of a single amino acid change at this position (Ile^{336} → Glu^{336}) resulted in only a 48% reduction. Replacement of Leu^{340} with Pro completely eliminated IpaC invasion function, whereas replacement with Glu only reduced invasion function 64% (Table II). The large negative effect of Pro replacement of amino acids near the C terminus of the putative IpaC coiled region, when compared with Glu substitution, is consistent with this region existing as a functionally important α-helix.

IpaC Nucleates Actin in Vitro—It has been reported that the IpaC homologue from *S. typhimurium* (SipC) nucleates actin *in vitro* (24). We find that IpaC also nucleates actin *in vitro* with an efficiency that is at least equal to that of SipC (Fig. 6).

TABLE II
The effect of site-specific proline residues within the predicted coiled-coil of IpaC on invasion function

Site-specific mutation	Relative invasion restored[a]
None	100 ± 15%
$Ile^{336} \rightarrow$ Glu (LE335)[b]	52 ± 6%
$Leu^{340} \rightarrow$ Glu (LE339)[b]	36 ± 8%
$Ser^{314} \rightarrow$ Pro	100 ± 14%
$Lys^{326} \rightarrow$ Pro	47 ± 5%
$Ile^{336} \rightarrow$ Pro	16 ± 3%
$Leu^{340} \rightarrow$ Pro	1 ± 0.3%

[a] Invasion was tested using a standard gentamycin protection assay. The data shown are from one representative experiment performs in triplicate ± S.E.

[b] The single amino acid substitutions were generated as part of the linker-scanning analysis using *Xho*I sites. LE335 replaced Leu^{335}-Ile^{336} with a Leu-Glu pair, and LE339 replaces Leu^{339}-Leu^{340} with a Leu-Glu pair.

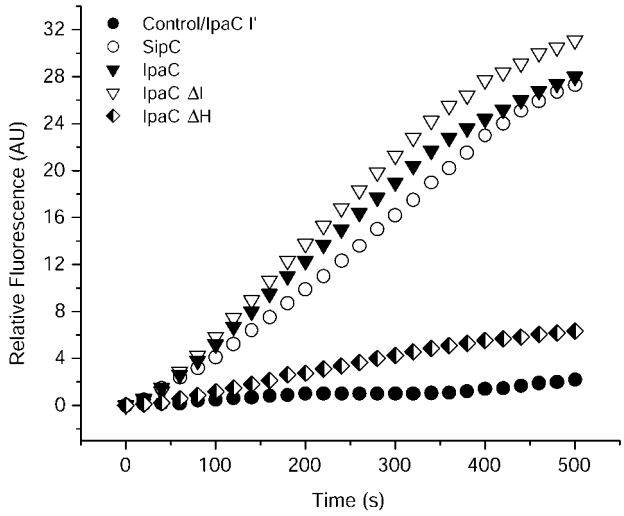

FIG. 6. **Actin nucleation was determined by incubating pyrene-actin with protein for 15 min followed by adding actin polymerization buffer.** Actin polymerization is monitored as an increase in pyrene fluorescence as a function of time, and this rate is greatly accelerated by actin-nucleating proteins such as SipC or IpaC relative to proteins that do not nucleate actin such as IpaC I′ or in the absence of added protein. Deletion of the IpaC C terminus (amino acids 171–363) also eliminates its actin nucleation activity (data not shown), whereas deletion of the N terminus up to amino acid 62 (IpaC ΔI) does not affect actin nucleation activity. Data shown are representative of multiple experiments. *AU*, arbitrary units.

Deletion of the IpaC N terminus does not affect this activity, whereas deletion of the C terminus (data not shown) or hydrophobic region does eliminate the ability of IpaC to nucleate actin (Fig. 6). Furthermore, the C-terminal addition of a 15-residue tag that eliminates IpaC effector function *in vivo* also eliminates the ability of IpaC to direct actin nucleation (data not shown), indicating that the C terminus of IpaC is required for actin nucleation.

DISCUSSION

IpaC is an essential participant in the invasion process of *S. flexneri* (3). It is involved in actin rearrangements, pathogen entry into phagosomal vacuoles, and the subsequent lysis of those vacuoles (2, 4). Although the broad functional organization of IpaC has been described (14, 29), little is known of the structure of the protein. We find that under physiological conditions, recombinant IpaC is composed of an α-helix (<10%), a β-sheet, and significant random structure (Table I). Thus, this protein may be considered a member of that recently recognized class of proteins whose native state contains a significant amount of disordered structure (30, 31).

Temperature perturbation studies show that IpaC undergoes a distinct structural transition involving both secondary and tertiary structure between 30 and 60 °C (Figs. 1 and 2). This does not involve complete unfolding since the majority of secondary structure is retained post-transition (Table I). Additionally, shifts in the derivative absorbance minima to shorter wavelengths, which would indicate exposure of buried aromatic resides to bulk solvent, were not observed. This conformational change is presumably related to temperature-induced aggregation of IpaC, as detected by turbidity measurements (Fig, 3, *top*). Two transitions are observed, the first between 30 and 70 °C and the second above 70 °C. This is consistent with the initial formation of soluble aggregates followed by more extensive aggregation and with previous observations that IpaC forms oligomers in solution (8). IpaC homotypic interaction involving the central hydrophobic region have also been detected using yeast two-hybrid analysis (32). The biologically relevant oligomerization state of IpaC is currently under investigation.

Examination of the N-terminal region of IpaC (IpaC I′) shows reduced structural content in comparison with the wild-type protein. This is accompanied by a reduced effect of temperature on the protein. IpaC I′ exhibits a small change in secondary structure above 30 °C (Fig. 1*C*), as well as a small tertiary structure transition between 30 and 60 °C (Fig. 2*F*). Differences in the environment of the aromatic residues of IpaC I′, detected as shifts in derivative absorbance wavelength when compared with that of IpaC, are also observed. These shifts may also reflect differences in aromatic amino acid content. IpaC contains three Phe residues, whereas only one is present in IpaC I′. Some limited oligomerization is also observed above 50–55 °C in this form of the protein (Fig. 3).

IpaC ΔH (residues 63–170 deleted) possesses significantly less ordered structure than IpaC, verging on a completely disordered conformation as shown by the shift of the CD minima from ~204 to 200 nm (Fig. 1*A*). No major temperature-dependent structural changes are observed for IpaC ΔH, although slight aggregation is apparent at higher temperatures. Thus, much of the disordered structure seen in the complete protein may be reflected in the behavior of this mutant.

The C terminus region of IpaC appears to contain the coiled-coil region postulated to contribute to IpaC self-interaction and effector function. Linker-scanning analysis provides an indirect picture of this region. A periodicity in loss of invasion activity is observed with different amino acid substitutions, which is consistent with functionally significant helical structure in this region (Fig. 5). Additional substitutions of proline residues, known helix breakers, also reduce invasion activity, further supporting this hypothesis.

During IpaC-mediated *Shigella* invasion of epithelial cells, IpaC is inserted into the host cytoplasmic membrane and, following uptake, mediates vacuolar escape (16), possibly by disrupting the phospholipid membrane following penetration (11). Previous studies have indicated that the ability to penetrate and disrupt liposomes occurs optimally when the lipid bilayer possesses a net negative charge (11). We find, however, that although interactions are enhanced in the presence of negatively charged liposomes, IpaC also causes low level disruption of neutral liposomes. The mechanism of disruption does not appear to be purely a detergent effect since at low temperatures and in the presence of neutral liposomes, the rate and extent of fluorescein release is much less than that observed by Triton disruption of liposomes. A strong temperature dependence is observed for the IpaC-liposome interaction for both lipid compositions. With negatively charged liposomes, the extent of release increases until the temperature reaches

~30 °C, at which point IpaC is nearly as effective in dye release as Triton. In contrast, neutral liposomes exhibit a sigmoidal temperature dependence in the release process. This may reflect the structural change occurring between 30 and 60 °C in IpaC, which may produce a more "penetration-efficient" form of IpaC. Alternatively, the concurrent aggregation process occurring in this temperature range may reflect the ability of oligomerized protein to disrupt the bilayer.

Neither IpaC I′ nor IpaC ΔH was able to disrupt liposomes. This is consistent with previous findings that the IpaC hydrophobic region is needed for association with Langmuir phospholipid monolayers (9). Coupled with the potential importance of the central hydrophobic region of IpaC for its overall stabilization, it is possible that this region contributes to overall tertiary structure stabilization, but when partially exposed, it directs penetration of phospholipid membranes. This is consistent with the results of ANS binding experiments in which titrations of IpaC with ANS at 40 °C demonstrate interaction of the dye with IpaC, indicating that hydrophobic regions of the protein become exposed under membrane-interactive conditions (not illustrated). As expected, little binding of ANS to the two mutants is seen over a wide temperature range.

IpaC ΔH and IpaC I′ fail to nucleate actin *in vitro*, whereas IpaC and IpaC ΔI nucleate actin efficiently (Fig. 6). This suggests that actin nucleation requires sequences at the IpaC C terminus; however, it is possible that conformational changes induced by mutations at the C terminus are responsible for this loss of activity. The IpaC C terminus contains a sequence predicted to form a coiled-coil that may be required for effector function. From these observations and linker-scanning studies that reinforce the coiled-coil hypothesis, it seems reasonable to conclude that this helical conformation is important for some aspect of actin nucleation. This is supported by preliminary data that the purified linker-scanning mutant AS339, which cannot direct *S. flexneri* invasion of cultured cells, is also unable to nucleate actin *in vitro* (not illustrated).

An analogous ability to nucleate actin was described for SipC of *S. typhimurium* (24); however, SipC has not been shown to act as a "direct effector" in *Salmonella* invasion. It was recently reported that SspC (SipC) from *S. typhimurium* co-purifies with HeLa cell actin in immunoprecipitation assays, but this relationship may be mediated by interactions with keratin 8 (33). Deletions introduced at the SspC C terminus and point mutations near its C terminus (most notably a Leu to Pro mutation) eliminate its ability to restore invasiveness to a *Salmonella* SspC mutant (33), suggesting similar structure-function relationships for the C termini of IpaC and SspC-(SipC). How such mutations affect the ability for SspC/SipC to nucleate actin are not known, but this warrants further study. In the same report, mutations at the C terminus of SspC caused the protein to no longer associate with HeLa cell membranes following incubation with *S. typhimurium* (33). How similar mutations influence the ability of IpaC to disrupt liposomes has yet to be determined.

As with *Salmonella*, the role of actin nucleation in invasion by *S. flexneri* is not immediately obvious. It is possible that IpaC-mediated actin nucleation: 1) contributes to the localization of actin polymerization in host cells (34, 35) or 2) permits the quick burst of actin polymerization needed for rapid entry. It is also possible that actin nucleation by IpaC has a more direct role in *Shigella* invasion. A recent report demonstrates that a *cdc42* knockout fibroblast-like cell line is still invaded by *S. flexneri*, albeit only at 15% of the levels seen in wild-type cells (36). Whatever its precise role, the IpaC protein is a key element in the invasion process of *S. flexneri* and may provide an important therapeutic target.

In conclusion, this work presents the first structural analysis of IpaC, based on the functional organization scheme presented previously (14). IpaC appears to be partially disordered with conformational lability increasing under physiological temperature. The existence of a helical domain at the C terminus of the protein, deemed necessary for effector function in the invasion process, is probed, and the presence of such a structure is strongly supported. Additionally, the interaction of IpaC with phospholipid bilayers is further characterized, and distinct domains of the protein are identified as necessary for this interaction. Finally, *in vitro* actin nucleation is demonstrated for IpaC, and this activity is preliminarily localized to the C terminus.

REFERENCES

1. Hale, T. L. (1991) *Microbiol. Rev.* **55,** 206–224
2. Centers for Disease Control and Prevention (2000) *Shigellosis*, www.cdc.gov/ncidod/dbmd/diseaseinfo/shigellosis_g.htm
3. Hueck, C. (1998) *Microbiol. Mol. Biol.* **62,** 379–433
4. Sansonetti, P. J., Ryter, A., Clerc, P., Maurelli, A. T., and Mounier, J. (1986) *Infect. Immun.* **51,** 461–469
5. Marquart, M. E., Picking, W. L., and Picking, W. D. (1996) *Infect. Immun.* **64,** 4182–4187
6. Menard, R., Prevost, M. C., Gounon, P., Sansonetti, P., and Dehio, C. (1996) *Proc. Natl. Acad. Sci. U. S. A.* **93,** 1254–1258
7. Tran Van Nhieu, G., Caron, E., Hall, A., and Sansonetti, P. J. (1999) *EMBO J.* **18,** 3249–3262
8. Davis, R., Marquart, M. E., Lucius, D., and Picking, W. D. (1998) *Biochim. Biophys. Acta* **1429,** 45–56
9. Tran, N., Serfis, A. B., Osiecki, J. C., Picking, W. L., Coye, L., Davis, R., and Picking, W. D. (2000) *Infect. Immun.* **68,** 3710–3715
10. De Geyter, C., Wattiez, R., Sansonetti, P., Falmagne, P., Ruysschaert, J. M., Parsot, C., and Cabiaux, V. (2000) *Eur. J. Biochem.* **267,** 5769–5776
11. De Geyter, C., Vogt, B., Benjelloun-Touimi, Z., Sansonetti, P. J., Ruysschaert, J. M., Parsot, C., and Cabiaux, V. (1997) *FEBS Lett.* **400,** 149–154
12. Kuwae, A., Yoshida, S., Tamano, K., Mimuro, H., Suzuki, T., and Sasakawa, C. (2001) *J. Biol. Chem.* **276,** 32230–32239
13. Terajima, J., Moriishi, E., Kurata, T., and Watanabe, H. (1999) *Microb. Pathog.* **27,** 223–230
14. Picking, W. L., Coye, L., Osiecki, J. C., Barnoski Serfis, A., Schaper, E., and Picking, W. D. (2001) *Mol. Microbiol.* **39,** 100–111
15. Blocker, A., Gounon, P., Larquet, E., Niebuhr, K., Cabiaux, V., Parsot, C., and Sansonetti, P. (1999) *J. Cell Biol.* **147,** 683–693
16. Osiecki, J. C., Barker, J., Picking, W. L., Serfis, A. B., Berring, E., Shah, S., Harrington, A., and Picking, W. D. (2001) *Mol. Microbiol.* **42,** 469–481
17. Picking, W. L., Mertz, J. A., Marquart, M. E., and Picking, W. D. (1996) *Protein Expression Purif.* **8,** 401–408
18. Provencher, S., and Glockner, J. (1981) *Biochemistry* **20,** 33–37
19. Sreerama, N., and Woody, R. (1990) *Anal. Biochem.* **209,** 32–44
20. Manavalan, P., and Johnson, W. C., Jr. (1987) *Anal. Biochem.* **167,** 76–85
21. Sreerama, N. *CDPro: A Software Package for Analyzing Protein Spectra*, lamar.colostate.edu/~sreeram/CDPro/index.html
22. Mach, H., and Middaugh, C. R. (1994) *Anal. Biochem.* **222,** 323–331
23. Avanti Polar Lipids, *Determination of Total Phosphorous*, www.avantilipids.com/DeterminationOfTotalPhosphorus.html.
24. Hayward, R. D., and Koronakis, V. (1999) *EMBO J.* **18,** 4926–4934
25. Mach, H., and Middaugh, C. R. (1993) *BioTechniques* **15,** 240–242
26. Mach, H., and Middaugh, C. R. (1995) *Biochemistry* **34,** 9913–9920
27. Silvius, J. R. (1982) in *Lipid-Protein Interactions* (Jost, P. C., and Griffith, O. H., eds), 2nd Ed., pp. 515, John Wiley & Sons, Inc., New York
28. Pallen, M. J., Dougan, G., and Frankel, G. (1997) *Mol. Microbiol.* **25,** 423–425
29. Barzu, S., Benjelloun-Touimi, Z., Phalipon, A., Sansonetti, P., and Parsot, C. (1997) *Infect. Immun.* **65,** 1599–1605
30. Dunker, A. K., Lawson, J. D., Brown, C. J., Williams, R. M., Romero, P., Oh, J. S., Oldfield, C. J., Campen, A. M., Ratliff, C. M., Hipps, K. W., Ausio, J., Nissen, M. S., Reeves, R., Kang, C., Kissinger, C. R., Bailey, R. W., Griswold, M. D., Chiu, W., Garner, E. C., and Obradovic, Z. (2001) *J. Mol. Graph. Model.* **19,** 26–59
31. Dunker, A. K., Brown, C. J., Lawson, J. D., Iakoucheva, L. M., and Obradovic, Z. (2002) *Biochemistry* **41,** 6573–6582
32. Page, A. L., Fromont-Racine, M., Sansonetti, P., Legrain, P., and Parsot, C. (2001) *Mol. Microbiol.* **42,** 1133–1145
33. Scherer, C. A., Cooper, E., and Miller, S. I. (2000) *Mol. Microbiol.* **37,** 1133–1145
34. Zhou, D. (2001) *Trends Microbiol.* **9,** 567–570
35. McGhie, E. J., Hayward, R. D., and Koronakis, V. (2001) *Trends Microbiol.* **9,** 569–570
36. Shibata, T., Takeshima, F., Chen, F., Alt, F. W., and Snapper, S. B. (2002) *Curr. Biol.* **12,** 341–345

Structure-Function Analysis of Invasion Plasmid Antigen C (IpaC) from *Shigella flexneri*

Lisa A. Kueltzo, John Osiecki, Jeff Barker, Wendy L. Picking, Baran Ersoy, William D. Picking and C. Russell Middaugh

J. Biol. Chem. 2003, 278:2792-2798.
doi: 10.1074/jbc.M208383200 originally published online November 8, 2002
